Journal of Chromatography A, 1399 (2015) 53–64

Contents lists available at ScienceDirect

Journal of Chromatography A

journal homepage: www.elsevier.com/locate/chroma

A critical evaluation of an asymmetrical flow field-flow fractionation system for colloidal size characterization of natural organic matter

Zhengzhen Zhou, Laodong Guo*

School of Freshwater Sciences, University of Wisconsin-Milwaukee, 600 East Greenfield Avenue, Milwaukee, WI 53204, USA

ARTICLE INFO

Article history:
Received 17 February 2015
Received in revised form 18 April 2015
Accepted 20 April 2015
Available online 27 April 2015

Keywords:
Flow field-flow fractionation
Dissolved organic matter
Colloidal size distribution
UV-absorbance
Fluorescence EEMs

ABSTRACT

Colloidal retention characteristics, recovery and size distribution of model macromolecules and natural dissolved organic matter (DOM) were systematically examined using an asymmetrical flow field-flow fractionation (AFlFFF) system under various membrane size cutoffs and carrier solutions. Polystyrene sulfonate (PSS) standards with known molecular weights (MW) were used to determine their permeation and recovery rates by membranes with different nominal MW cutoffs (NMWCO) within the AFlFFF system. Based on a ≥90% recovery rate for PSS standards by the AFlFFF system, the actual NMWCOs were determined to be 1.9 kDa for the 0.3 kDa membrane, 2.7 kDa for the 1 kDa membrane, and 33 kDa for the 10 kDa membrane, respectively. After membrane calibration, natural DOM samples were analyzed with the AFlFFF system to determine their colloidal size distribution and the influence from membrane NMWCOs and carrier solutions. Size partitioning of DOM samples showed a predominant colloidal size fraction in the <5 nm or <10 kDa size range, consistent with the size characteristics of humic substances as the main terrestrial DOM component. Recovery of DOM by the AFlFFF system, as determined by UV-absorbance at 254 nm, decreased significantly with increasing membrane NMWCO, from 45% by the 0.3 kDa membrane to 2–3% by the 10 kDa membrane. Since natural DOM is mostly composed of lower MW substances (<10 kDa) and the actual membrane cutoffs are normally larger than their manufacturer ratings, a 0.3 kDa membrane (with an actual NMWCO of 1.9 kDa) is highly recommended for colloidal size characterization of natural DOM. Among the three carrier solutions, borate buffer seemed to provide the highest recovery and optimal separation of DOM. Rigorous calibration with macromolecular standards and optimization of system conditions are a prerequisite for quantifying colloidal size distribution using the flow field-flow fractionation technique. In addition, the coupling of AFlFFF with fluorescence EEMs could provide new insights into DOM heterogeneity in different colloidal size fractions.

1. Introduction

Natural dissolved organic matter (DOM) in aquatic systems is one of the largest reduced carbon pools and plays an important role in the biogeochemical cycling of carbon, nutrients, trace metals and organic contaminants [1–5]. The bulk DOM is a heterogeneous mixture containing both dissolved and colloidal organic matter with a range of sizes or molecular weights and chemical characteristics [6–8]. Colloids have been shown to comprise a considerable fraction of the bulk DOM and to act as the intermediary between dissolved and particulate phases, critically regulating the fate, transport and bioavailability of organic and inorganic chemical species in aquatic systems [9–11]. Nevertheless, knowledge on size distribution and chemical composition of dissolved and colloidal organic matter remains scarce.

The applications of ultrafiltration techniques have advanced our understanding of aquatic colloids [12,13]. However, ultrafiltration only gives a single cutoff separation for a specific colloidal size fraction. Flow field-flow fractionation (FlFFF), on the other hand, is able to provide continuous size separation and characterization of colloidal materials [14]. The FlFFF instrument mainly consists of a separation chamber and an ultrafiltration membrane installed on the bottom of the channel. The pore size of the ultrafiltration membrane represents the lower-cutoff of the analyzed colloids [15]. The perpendicular cross flow is applied to provide a retention field. Based on the diffusion coefficients, which can be deferred to the sizes given calibrated correlation between size and diffusion coefficient, of colloids, they are equilibrated at corresponding positions in the retention field [16]. Since the thickness of the FlFFF channel is in the order of a few hundred μm, the channel flow is parabolic, eluting materials distributed at different perpendicular positions

* Corresponding author. Tel.: +1 414 382 1742; fax: +1 414 382 1705.
E-mail address: guol@uwm.edu (L. Guo).

http://dx.doi.org/10.1016/j.chroma.2015.04.035
0021-9673/

at different time [17]. Essentially, smaller colloids are eluted faster due to their larger diffusion coefficient and ability to diffuse further against the retention field, while larger colloids would be eluted later [18]. When coupled with online detectors, FlFFF could provide simultaneous separation and characterization of aquatic colloids and nanoparticles [14,19,20]. Due to its easier maintenance and handling and see-through channel [21–23], asymmetrical FlFFF (AFlFFF) has been widely used in colloidal characterization of natural DOM in aquatic environments, including seawater [24–26], river water [27,18,28], soil [29], and others [23].

Using FlFFF, previous studies have reported size distributions and composition of natural DOM, with MWs ranging from a few hundred to a few thousand Dalton (Da) and organic molecules from uric acids to humic materials and proteins [30–33]. Interestingly, eluted colloidal organic matter from FlFFF channel could still contain DOM with MWs smaller than the membrane nominal molecular weight cutoff (NMWCO), as shown in many previous studies, which have been attributed to electrostatic repulsion [15–17,34,35]. On the other hand, recoveries of DOM by FlFFF systems are generally much lower than 50% even under optimized conditions [36,26], indicating that a great proportion of DOM could be lost, most likely through the membrane during the on-channel preconcentration (sample focusing) process. Furthermore, different membranes with different NMWCOs and membrane materials have been used in different FlFFF systems, making data interpretation and comparisons between studies difficult. Quantitative understanding of retention and permeation characteristics of colloidal and macromolecular organic matter during FlFFF separation under different membranes and other system settings is largely lacking.

In the present study, polystyrene sulfonate (PSS) standards with known MWs were used to determine their permeation and rejection characteristics by membranes with different NMWCOs and in turn to calibrate the membrane's NMWCO within our AFlFFF system. Using the well-calibrated membranes, the recovery rates and colloidal size distribution of model macromolecular standards and natural DOM samples were then quantitatively evaluated to examine the effect of membrane MWCOs. In addition, the effect of different system settings such as membranes and carrier solutions (different pH, matrix and ionic strength) were examined for optimization of the AFlFFF system and characterization of natural DOM. The AFlFFF system was further coupled off-line with the fluorescence excitation-emission matrix (EEM) technique to evaluate the heterogeneity in DOM characteristics among different size ranges.

2. Materials and methods

2.1. Instrumentation, membrane, and flow setting

A flowchart showing procedures using our AFlFFF system (AF2000, Postnova, Salt Lake City, UT) is shown in Fig. 1. Our AFlFFF system was coupled online with a UV-absorbance detector (SPD-20A, Shimadzu, Tokyo, Japan) set at 254 nm and two fluorescence detectors (RF-20A, Shimadzu, Tokyo, Japan) with Ex/Em wavelengths at 350/450 nm and 275/340 nm, respectively, to provide size distribution of colloids targeting at chromophoric, humic-like and protein-like DOM, respectively (Fig. 1). Another online detector, a multi-angle light scattering (MALS) detector (AF2000, Postnova, Salt Lake City, UT), was also used to provide additional information for colloidal size partitioning. Furthermore, our AFlFFF system was coupled offline with a 3D fluorescence spectrophotometer to examine DOM composition change among different colloidal size fractions through their excitation-emission matrices (Fig. 1). Hereafter, the word "fractogram" is adopted to refer to the detected signals as a function of the retention time from AFlFFF analysis [37,38,28].

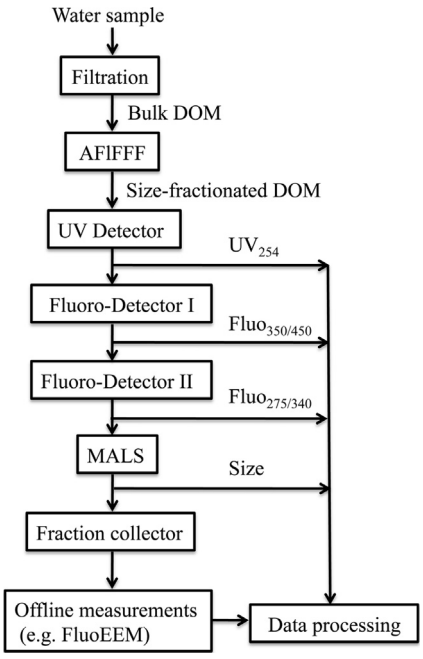

Fig. 1. Flowchart for sample analysis using the asymmetrical flow field-flow fractionation (AFlFFF) system. Our AFlFFF system was coupled online with a UV-absorbance detector set at 254 nm (UV_{254}), two fluorescence detectors set at Ex/Em 350/450 nm for humic-like ($Fluo_{350/450}$) and Ex/Em 275/350 nm for protein-like ($Fluo_{275/340}$) DOM, respectively, and a multi-angle light scattering (MALS) detector to examine the size of DOM, as well as off-line with a spectrofluorometer to acquire fluorescence excitation-emission matrices (EEMs) data.

Three membranes with different manufacturer-rated NMWCOs were used with our AFlFFF system for membrane calibration and sample analysis, including the 0.3 kDa polyether sulfone, 1 kDa polyether sulfone, and 10 kDa regenerated cellulose membranes (all from Postnova, Salt Lake City, UT). For measurements of macromolecular standards and samples, a 1 mL injection volume was consistently used for on-channel pre-concentration of samples. During the pre-concentration, dissolved and colloidal organic matter with size larger than the membrane cutoff should be retained by the membrane and later being eluted to the detectors, and the permeable fractions should penetrate through the membrane being carried to waste. Table 1 lists the flow settings of the AFlFFF system used with different membranes. Notice that flow settings between the 0.3 kDa and the 1 and 10 kDa membrane systems were slightly different. These flow rates provided >95% recovery of macromolecular standards and optimal colloidal separation in the size range of 0.5–40 nm with ~50 min fractionation time. Initially, a 15 mmol L^{-1} $NaCl_{(aq)}$ solution was used as the carrier solution during membrane NMWCO calibration. In order to examine the effect of carrier solutions on the recovery of DOM by the AFlFFF system, three carrier solutions were tested: 1) 15 mmol L^{-1} $NaCl_{(aq)}$ with pH = 6; 2) 15 mmol L^{-1} $NaCl_{(aq)}$ with pH = 8 (adjusted with NaOH); and 3) a mixed solution with 10 mmol L^{-1} $NaCl_{(aq)}$ and 5 mmol L^{-1} $H_3BO_{3(aq)}$ and pH of 8 (adjusted with NaOH), which were denoted as Carrier 1, Carrier 2, and Carrier 3, respectively (Table 2). Sodium chloride was purchased from Fisher Scientific (99.8%, Fair Lawn, NJ). Boric acid was from Amresco Inc. (ACS Grade, Solon, Ohio). Sodium hydroxide was acquired from VWR International, LLC. (ACS Grade, Radnor, PA). Ultrapure water was prepared from building-based osmosis-deionized water through a Purelab flex water system (ELGA Labwater LLC., UK). The final E-pure water had a conductivity of 18.2 MΩ and a TOC concentration of 1 ppb or 1 μg-C/L.

Table 1
Flow settings used for the AFlFFF system.

	Tip (mL/min)	Focus (mL/min)	Cross (mL/min)	Detector (mL/min)
For 1 kDa and 10 kDa membranes				
Focusing step	0.20	4.30	4.00	0.50
Elution step	4.50		4.00	0.50
For 0.3 kDa membrane				
Focusing step	0.10	2.10	1.50	0.70
Elution step	2.20		1.50	0.70

Table 2
A list of carrier solutions used.

	Composition	pH	Ionic strength (mmol L^{-1})
Carrier 1	15 mmol L^{-1} $NaCl_{(aq)}$	6	15
Carrier 2	15 mmol L^{-1} $NaCl_{(aq)}$, pH = 8 (adjusted with NaOH)	8	15
Carrier 3	10 mmol L^{-1} NaCl and 5 mmol L^{-1} $H_3BO_{3(aq)}$, pH = 8 (adjusted with NaOH)	8	10.3

2.2. Calibration of AFlFFF system and membrane cutoff

A series of protein standards (all from Sigma Aldrich, St. Louis, MO) with known MWs and diffusion coefficients, as listed in Table 3, were used to calibrate the AFlFFF system and to establish a relationship between system retention time and diffusion coefficient of colloids under chosen instrument conditions, such as membrane MWCOs, carrier solutions and flow settings. Based on the established relationship, the retention time of macromolecules or natural DOM can be readily converted to diffusion coefficient and later hydrodynamic diameter using the Stokes law ([26] and references therein). Further, a series of PSS standards (Scientific polymer products, Inc., Ontario, NY) with known MWs (Table 3) were used to establish a relationship between determined diffusion coefficients and MWs following the equation below:

$$D = AM^{-b}$$

where D is diffusion coefficient, M is molecular weight and A and b are constants for a particular sample-solvent system [15,14]. Based on this relationship, MWs could be converted from diffusion coefficients to obtain samples' colloidal size distribution in terms of molecular weights. Quinine sulfate (Sigma Aldrich, St. Louis, MO) solutions ranging from 0 to 100 ppb were used to quantify the concentration of macromolecules or natural DOM samples, expressed in quinine sulfate equivalent units (ppb-QSE), converted from detectors' signal intensity [28,39].

For membrane's MWCO calibration, a series of PSS standards and Rhodamine B (Sigma Aldrich, St. Louis, MO), as listed in Table 3, were used to examine their permeation and rejection characteristics by each AFlFFF membrane and to determine each membrane's apparent NMWCO based on a ≥90% recovery rate [40,41]. The recovery or retention rate (R%) was determined by normalizing signal peak area of a fractionation sample-run (A), where there was a focusing process and the cross-flow field was applied for retention, to that of a non-fractionation sample-run (A_0), where focus flow and cross flow were absent and only tip flow was applied (e.g. [42]), as in the equation:

$$R\% = \left(\frac{A}{A_0}\right) \times 100\%$$

2.3. Measurements of natural DOM samples

After the calibration of the AFlFFF system and membrane, a mixture of PSS standards was first used to demonstrate sequential elution and separation of colloids, including 1.6 kDa PSS (53 mg L^{-1}), 16 kDa PSS (36 mg L^{-1}), 127 kDa PSS (60 mg L^{-1}), and 505 kDa PSS (113 mg L^{-1}). Two soil DOM samples (SDOM-A and SDOM-B) were measured with the AFlFFF system using the three different membranes to examine their colloidal size distributions and the effect of membrane NMWCO on the recovery of DOM from the AFlFFF system. Both soil leachates were acquired by leaching ~100 g of each soil with ~500 mL of 18.2 MΩ pure water overnight, and then filtered through pre-combusted 0.7 μm glass-fiber filters (GF/F, Whatman, Piscataway, NJ) before measurements. In addition, the PSS mixture and a riverine water sample were analyzed to examine the effect of carrier solutions on the recovery rate and elution time of PSS and natural DOM. The river water sample was filtered with 0.4 μm polycarbonate Nuclepore filters (Whatman, Piscataway, NJ) and the filtrate was collected for AFlFFF analysis.

During the analysis of soil DOM sample (SDOM-B) on the AFlFFF system, size-fractionated samples were also collected at three different colloidal size ranges at the 0.5–4 nm, 4–8 nm and

Table 3
A list of protein standards (all from Sigma Aldrich, St. Louis, MO) used for calibrating the AFlFFF system (conversion of retention time into diffusion coefficient and hydrodynamic diameter) and Rhodamine B (Sigma Aldrich, St. Louis, MO) and polystyrene sulfonate (PSS) standards (Scientific Polymer Products, Inc. Ontario, NY) for the calibration of membrane's molecular weight cutoff (MWCO, based on a ≥90% recovery) of the AFlFFF system (conversion of diffusion coefficient into molecular weight).

Protein	Molecular weight (Dalton)	Hydrodynamic diameter (nm)	Diffusion coefficient (m^2 s^{-1})	Purity or grade
Cytochrome *C*	12,400	3.302	1.3×10^{-10}	≥95%
α-Chymotrypsinogen A	25,000	4.528	9.5×10^{-11}	6×crystallization
BSA	66,000	6.979	6.2×10^{-11}	≥98%
Ferritin	443,000	11.89	3.6×10^{-11}	Saline solution sterile-filtered
Thyroglobulin	669,000	16.45	2.6×10^{-11}	≥90%
Rhodamine B	479	–	–	≥95%
PSS 1.6	1640	–	–	–
PSS 4.9	4950	–	–	–
PSS 16	16,000	–	–	–
PSS 34	34,700	–	–	–
PSS127	127,000	–	–	–
PSS 505	505,100	–	–	–

>55 nm for the acquisition of EEM data using a spectrofluorometer (Fluoromax-4, Horiba Scientific, Edison, NJ) following procedures described in [43].

2.4. Statistics

Non-linear regressions between the molecular weights of standards and their recovery rates were performed using Sigma-Plot software (Systat Software, Inc., San Jose, CA). Fitted equations with the highest r-squared values and lowest standard errors of estimates were finally chosen, which are exponential rise to maximum, double, 5 parameter for data for the 0.3 kDa membrane, hyperbola, single rectangular I, 3 parameter for 1 kDa and exponential rise to maximum, single, 3 parameter for 10 kDa sample sets.

3. Results and discussion

3.1. Relationship between retention time and macromolecular sizes

Separation and overall performance of the AFlFFF system with different membranes were calibrated using a series of protein standards and mixed PSS macromolecules (Table 3). Linear correlations between the retention time and reciprocal of diffusion coefficient of protein standards were established for all three membranes, including the 0.3 kDa polyether sulfone ($r^2 = 0.997$, $p < 0.0001$), 1 kDa polyether sulfone ($r^2 = 0.945$, $p = 0.0005$), and 10 kDa regenerated cellulose ($r^2 = 0.992$, $p < 0.0005$) membranes (Fig. 2). These results indicated that the AFlFFF system indeed responded linearly

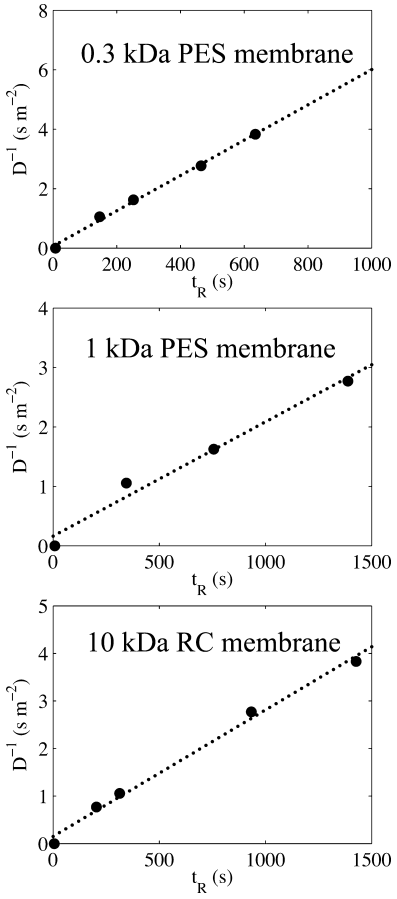

Fig. 2. Correlations between retention time of protein standards and reciprocal of their diffusion coefficient for three different membranes, including the 0.3 kDa and 1 kDa polyether sulfone membranes (PSE), and the 10 kDa regenerated cellulose (RC) membrane.

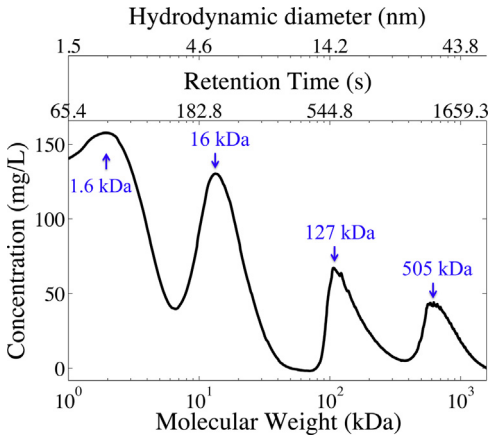

Fig. 3. Simultaneous separation of macromolecular PSS mixture, including 1.6 kDa PSS (53 mg L^{-1}), 16 kDa PSS (36 mg L^{-1}), 127 kDa PSS (60 mg L^{-1}), and 505 kDa PSS (113 mg L^{-1}), by the AFlFFF system using a 0.3 kDa PES membrane showing continuous elution of different sized colloids under optimal flow settings.

between retention time and reciprocal of diffusion coefficient or hydrodynamic diameter of macromolecules over the size range between 3 nm and 16 nm, conforming to the FlFFF theory. Thus, reliable performance, separation and size determination in this size range could be achieved.

To further demonstrate the ability of the AFlFFF system under assigned settings to perform continuous size separation of colloidal macromolecular materials, a mixture of macromolecular standards consisting of 1.6 kDa, 16 kDa, 127 kDa, and 505 kDa PSS (Table 3) was analyzed using the AFlFFF equipped with the 0.3 kDa membrane under experimental settings listed in Table 1. Notice that the PSS standards used here all have a MW (1.6–505 kDa) well above the membrane's NMWCO of 0.3 kDa. As shown in Fig. 3, the four PSS standards were sequentially eluted and separated following their orders of hydrodynamic diameter and molecular weight. However, in the fractogram the first peak of the 1.6 kDa PSS was not clearly separated from the void peak, likely resulting from overloading effect due to the injection of high concentration mixed PSS standards. With analyzed samples that are low in concentrations, the separation from the void peak became clear (see fractograms in Figs. 6 and 8). Secondly, peaks of the 127 kDa and 505 kDa PSS appeared less symmetrical comparing from the smaller standards in the fractogram, likely due to the relatively extended interactions between the PSS standards and the ultrafiltration membrane during their separation process. The same asymmetrical fractogram of 505 kDa PSS standard was also present when analyzed alone and when analyzed using different membranes and flow rates (data not shown). To minimize the adverse effects from the interactions between analytes and/or between analytes and the membrane, one could tune the AFlFFF system settings to target on the larger colloidal size within a narrower size window, thus shortening the time of analysis and lessening the interaction between colloids and the membrane. Overall, the AFlFFF system operated under the assigned flow settings and the specific membrane (0.3 kDa here) seems capable of simultaneous separation and characterization of samples containing complex mixture of macromolecular substances and thus natural dissolved and colloidal organic matter. These optimal system settings and conditions were then used for further calibration and sample analysis reported in the following sections.

3.2. Retention characteristics of macromolecular organic matter by AFlFFF system with different membranes

A series of PSS standards were analyzed with the AFlFFF system to examine their retention characteristics and to determine

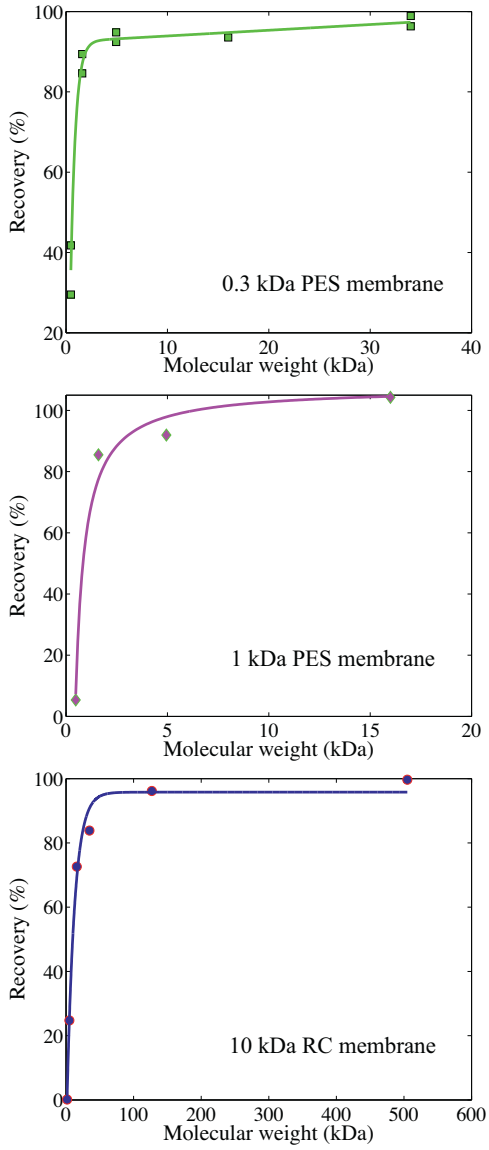

Fig. 4. Variations in recoveries of different macromolecular standards by three different membranes with different NMWCOs, including the 0.3 kDa (upper panel), 1 kDa (middle panel) and 10 kDa (lower panel) membranes. Recoveries at 90% are used to derive membrane's apparent MWCO (see Table 3).

the membranes' apparent MWCOs and compare with the manufacturer's cutoff ratings. As shown in Fig. 4, the recovery or retention rates of macromolecules by all three membranes increased with increasing molecular weight or size from Rhodamine B to different PSS standards. For each membrane, recoveries of the macromolecular standards varied from as low as near 0% for the lowest MW standard (0.47 kDa Rhodamine B or 1.6 kDa PSS) to as high as close to 100% for the highest MW standard used (16, 34, or 505 kDa PSS).

From the relationships between the molecular weights and the recoveries of macromolecular standards, the apparent MWCO of a specific membrane can be determined based on a ≥90% recovery [40,41]. As shown in Table 4, the apparent MWCOs for the three ultrafiltration membranes were determined to be 1.9 kDa for the 0.3 kDa, 2.7 kDa for the 1 kDa, and 33 kDa for the 10 kDa membranes, respectively. These apparent MWCOs are all significantly larger than their respective manufacturer's NMWCO, with a difference in the cutoffs ranging from 1.6 kDa for the 0.3 kDa membrane to about 23 kDa for the 10 kDa membrane. Indeed, significant differences in ultrafiltration membrane's cutoffs between manufacturer's rating and laboratory evaluation have been reported [44,45], although no significant difference in membrane cutoffs was also observed depending on specific membrane [40]. These results demonstrate the importance in examining the retention characteristics of ultrafiltration membranes within an AFlFFF system, especially when membranes are in prolonged use, and in determining the actual MWCO for the separation and characterization of colloidal materials that are close in size to the membrane's NMWCO. Since natural DOM contains mostly organic materials less than 10 kDa [46,12] and the average MWs of humic substances are at the 2–3 kDa size range [31,47], it is imperative to know what colloidal size ranges are of significance in different samples and what specific membrane's MWCO should be used in an AFlFFF system for colloidal size characterization.

3.3. Recovery rates of colloidal organic matter by different membranes

Using the calibrated AFlFFF system and membranes, two soil leachate samples (SDOM-A and SDOM-B) were analyzed to characterize the DOM recovery and colloidal size distribution under different membrane NMWCOs. The recoveries (%) of chromophoric (quantified by $UV_{254\,nm}$), humic-like ($Fluo_{350/450\,nm}$) and protein-like ($Fluo_{275/340\,nm}$) DOM in the two soil leachate samples using the three different membranes are listed in Table 5. For both samples, the recoveries of chromophoric, humic-like and protein-like DOM all consistently decreased as the membranes' NMWCO increased from 0.3 kDa to 1 kDa, and to 10 kDa (Table 5 and Fig. 5). For example, 24% and 45% of chromophoric DOM in the two soil leachates respectively were retained by the AFlFFF system with the 0.3 kDa membrane. These recoveries are comparable to the retention rates of peat soil and swamp DOM samples acquired from cross-flow ultrafiltration methods with a 1 kDa membrane [2,48], indicating similar sample recoveries could be achieved between the AFlFFF and ultrafiltration. However, only 5–9% of the chromophoric DOM in the two soil DOM samples was retained by the 1 kDa membrane, and the recovery rates dropped to 2–3% using the 10 kDa membrane (Table 5). Similarly, for humic-like organic components of the two soil leachate samples, the recoveries were 24–34% by the 0.3 kDa membrane, 3–4% by the 1 kDa membrane, and 0.03–0.1% by the 10 kDa membrane (Table 5). For protein-like organic components in the two soil leachate samples, the recoveries were 12–30% by the 0.3 kDa membrane, 3–18% by the 1 kDa membrane, and 1–13% by the 10 kDa membrane (Table 5), again showing a rapid decrease in

Table 4
Ultrafiltration membranes used in the AFlFFF system and comparisons between manufacturer's rated NMWCO (kDa) and calibrated results based on a ≥90% recovery rate of PSS standards (see Fig. 4). NMWCO denotes nominal molecular weight cutoff.

	Postnova 0.3 kDa	Postnova 1 kDa	Postnova 10 kDa
Manufacturer's rating (kDa)	0.3	1.0	10
Material	Polyether sulfone	Polyether sulfone	Regenerated cellulose
Calibrated NMWCO (kDa)	1.9	2.7	33
Difference between manufacturer's rating and actual cutoff (kDa)	1.6	1.7	23

Table 5
Recoveries (%) of chromophoric (UV_{254}), humic-like ($Fluo_{350/450}$) and protein-like ($Fluo_{350/450}$) components in two soil dissolved organic matter samples (DOM-A and DOM-B) by the AFlFFF system with different membranes.

	Soil DOM-A			Soil DOM-B		
	UV_{254}	$Fluo_{350/450}$	$Fluo_{275/340}$	UV_{254}	$Fluo_{350/450}$	$Fluo_{275/340}$
0.3 kDa	24	24	12	45	34	30
1 kDa	5	4	3	9	3	18
10 kDa	3	0.03	1	2	0.1	13

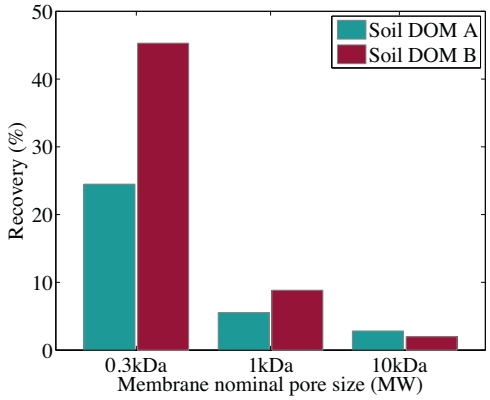

Fig. 5. Examples showing decreasing colloidal recoveries (%) with increasing membrane NMWCO for chromophoric (UV_{254}) DOM in soil leachate samples.

DOM recovery with increasing membrane's NMWCO. Significant DOM losses during the on-channel pre-concentration (or sample focusing) phase were largely the result of DOM permeation through the membrane. During the sample focusing step, large quantities of carrier solution would be introduced to the AFlFFF system and the permeable DOM fractions were carried to the waste. As the membrane pore size increases, the molecular size of the permeable fraction would also increase, resulting in a higher loss of DOM materials.

Fractograms of the SDOM-B sample using the three different membranes were further used to quantify DOM size partitioning to different size intervals in the whole colloidal size spectrum. Over 48–70% of the chromophoric DOM was partitioned to the <2 nm colloidal size fraction when the 0.3 kDa or 1 kDa membrane was used, while only 9% of the chromophoric DOM was partitioned to the <2 nm colloidal fraction when the 10 kDa membrane was used within the AFlFFF system (Table 6). The variation in both the recoveries and colloidal size partitioning between membranes clearly indicate that larger fractions and more smaller sized DOM can be retained by the 0.3 kDa or 1 kDa membrane, but were lost when using the 10 kDa membrane (Fig. 5).

As shown in Table 6, regardless of the membrane's cutoffs used, over 83–97% of the chromophoric DOM was present in the <5 nm colloidal size fraction in the SDOM-B sample (Table 6). This is consistent with the fact that natural humic-like DOM is small in size and has an average MW of ~2–5 kDa [15,21,49]. Our previous studies using FlFFF systems have also identified the partitioning of chromophoric and humic-like DOM mostly to the 0.5–3 nm size range, or smaller than 10 kDa [28,26,39]. Additionally, in both soil leachate samples, the recoveries of humic-like DOM was consistently lower than the chromophoric DOM components, especially when larger (1 kDa and 10 kDa) NMWCO membranes were used (Table 6). Similar results showing lower recovery of humic-like DOM as compared with chromophoric DOM have also been reported by Zanardi-Lamardo et al. [42] and Stolpe et al. [26], supporting a smaller size partitioning of humic-like material as compared with the bulk chromophoric DOM. Protein-like DOM, in contrast, showed a much smaller variability in recovery rates as compared with those of chromophoric and humic-like DOM components between membranes (Table 5 and Fig. 5), due to its more complex nature and relatively larger size range (>20 nm) [39].

Overall, lower recoveries for natural DOM by AFlFFF systems when using the 10 kDa or 1 kDa NMWCO membranes are mainly due to the characteristics in size distribution and organic composition with mostly humic substances and consequently the loss of lower MW DOM components through the membrane during the on-channel pre-concentration (focusing) phase. Thus, when a 1 kDa or 10 kDa membrane was used for AFlFFF analysis of natural DOM, it is likely to result in low recovery and underestimation of colloidal materials at smaller size ranges, leading to biased DOM size distributions. If one is interested in the whole size distribution of dissolved and colloidal organic matter, membranes with smaller NMWCOs (e.g. 0.3 kDa, the currently smallest cutoff available) are highly recommended for size separation and characterization of natural DOM samples using AFlFFF techniques.

3.4. Effect of membrane cutoff on DOM fractograms

The fractograms of natural DOM are depicted in Fig. 6, showing their variations and shift in size distributions under different membrane MWCOs for chromophoric, humic-like, and protein-like colloidal components in the 0.5–10 nm size range for a soil leachate sample (SDOM-B). All DOM components (chromophoric, humic-like and protein-like) smaller than 1 nm (~1 kDa) were detectable using the 0.3 kDa membrane, while materials slightly larger than 1 nm (~1 kDa) began to show their presence when the 1 kDa membrane was employed, and only materials larger than 1.5 nm (~2.5 kDa) could be seen in the fractograms using the 10 kDa

Table 6
Differences in the AFlFFF-measured concentration and relative percentage in the bulk dissolved phase of chromophoric DOM in a soil DOM sample (SDOM-B), as determined from UV absorbance at 254 nm, in different size intervals, showing more chromophoric DOM detected at the 0.5–1 nm size range when the 0.3 kDa membrane was used.

Size range	Concentration of chromophoric DOM in different size intervals (μg/L)			Percentage (%) of chromophoric DOM in each size interval within the AFlFFF-recoverable size range		
	0.3 kDa membrane	1 kDa membrane	10 kDa membrane	0.3 kDa membrane	1 kDa membrane	10 kDa membrane
0.5–1 nm	73,183	6947	0	11	4	0
1–1.5 nm	124,104	51,947	0	18	30	0
1.5–2 nm	133,041	62,604	3874	19	36	9
2–5 nm	285,195	46,882	32,708	41	27	74
5–35 nm	24,677	2060	5560	4	1	13
35–700 nm	45,973	4150	1842	7	2	4

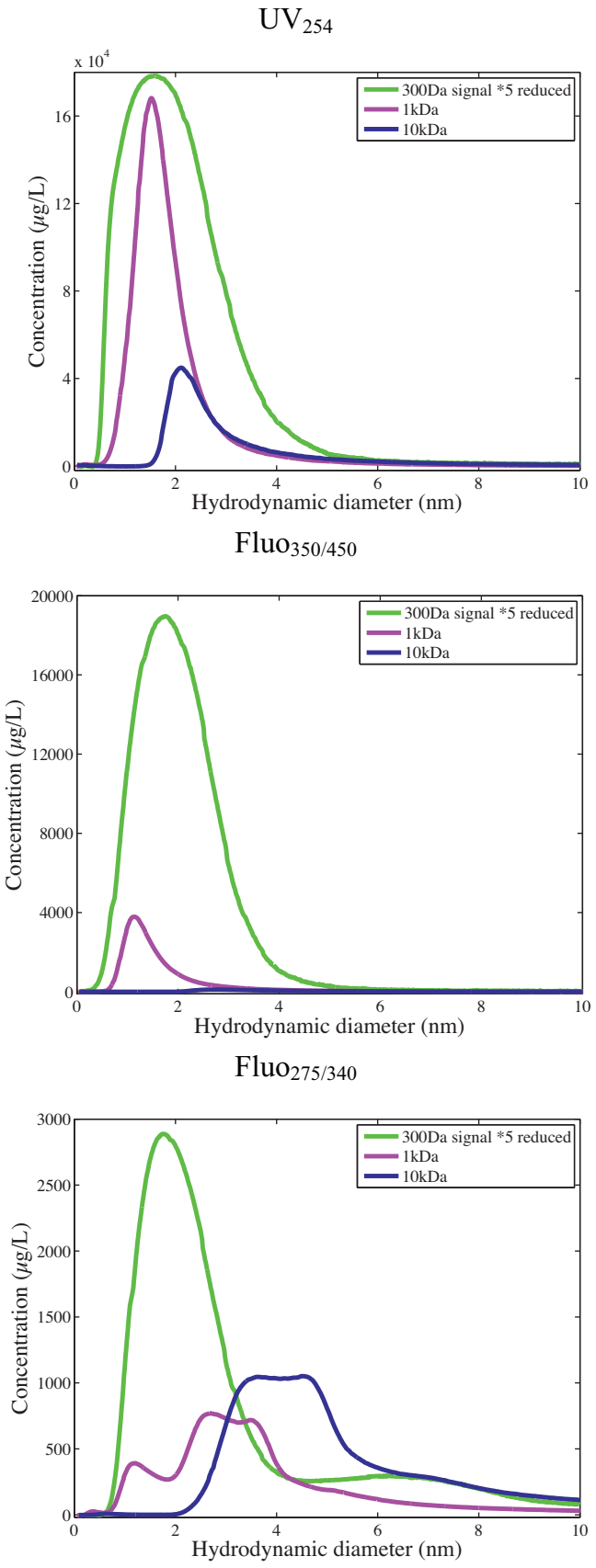

Fig. 6. Changes in fractograms of chromophoric (UV_{254}), humic-like ($Fluo_{350/450}$) and protein-like ($Fluo_{275/340}$) substances in a soil leachate sample (SDOM-B).

membrane (Fig. 6). As expected, both chromophoric and humic-like DOM components recovered by both the 1 kDa and 10 kDa membranes are included in, or part of, the size spectrum derived from the 0.3 kDa membrane. In other words, DOM components recovered by the 1 or 10 kDa membrane are only a subset of DOM components recovered by the 0.3 kDa membrane, consistent with the progressive decrease in DOM recoveries with increase membrane cutoff shown in Table 6 and Fig. 5. For the protein-like DOM components, the relative importance of each size range recovered by different membranes was not as consistent as those observed for chromophoric and humic-like DOM components (Fig. 6), likely due to the surface active nature of protein-like DOM and its interactions with membranes or coagulation effect since the same sample has been stored for a couple of months in refrigerator (4 °C) between its measurements with AFlFFF using the 10 kDa and 0.3 kDa membranes, respectively.

DOM partitioning to different size intervals was quantified via the integration of the fractograms over specific size ranges. Table 6 shows the integrated concentrations of chromophoric DOM at each size interval, as well as their corresponding percentages in the whole AFlFFF-recoverable size range. For example, the concentration of the 0.5–1 nm colloidal size range decreased from 73,183 ppb-QSE for the 0.3 kDa membrane to 6947 ppb-QSE for the 1 kDa and undetectable for the 10 kDa membrane, respectively (Table 6). Also, the percentage of chromophoric DOM in the 0.5–1 nm size range decreased from 11% for the 0.3 kDa membrane to 4% for the 1 kDa and was undetectable for the 10 kDa membrane (Table 6). The integrated concentration of AFlFFF-recoverable materials at the 0.5–5 nm size range also decreased with increasing membrane cutoff, varying from 615,523 ppb-QSE to 168,380 and to 36,582 ppb-QSE for the 0.3 kDa, 1 kDa and 10 kDa membranes, respectively, for the chromophoric DOM components (Table 6). As discussed in Section 3.3, the AFlFFF-recoverable colloids decreased when membrane NMWCO increased from 0.3 to 10 kDa. Consistent with results shown in Fig. 6 and Table 6, the decline in DOM recovery was again mostly the result of the loss of smaller colloidal materials partitioning to the 0.5–5 nm size range. Since natural DOM mostly partitions to the 0.5–5 nm size range, the 0.3 kDa membrane is much more favorable to achieving higher recovery and representative DOM size distributions.

3.5. *Effect of carrier solutions on sample recovery and elution time*

Three different carrier solutions, as listed in Table 2, were used to examine the variations in recoveries and elution times of a standard PSS mixture sample and a riverine DOM sample under the same AFlFFF operational conditions using the 0.3 kDa PES membrane (Table 1). For the PSS mixture, recoveries of chromophoric DOM were 83%, 82% and 97% when the Carriers 1, 2 and 3 were used respectively, showing the highest recovery with Carrier 3 (Fig. 7). The change in the recovery of humic-like DOM was insignificant, i.e., 83%, 84% and 85% for the Carriers 1, 2 and 3, respectively (Fig. 7). Protein-like DOM showed a similar variation trend as chromophoric DOM and had recoveries of 77%, 76%, and 82% for the Carriers 1, 2 and 3, respectively (Fig. 7). Generally, relatively higher recovery of PSS mixture was achieved when Carrier 3 was used. Compared to the PSS mixture sample, the overall recovery of the riverine DOM was much lower. Chromophoric DOM had recoveries of 31%, 31% and 30% for the Carriers 1, 2 and 3, respectively, showing negligible effect from different carrier solutions. Similarly, recoveries of humic-like DOM also change little for different carrier solutions, 15%, 16% and 15% for the Carriers 1, 2 and 3, respectively. For protein-like DOM components, however, effect of carrier solutions on the recovery was more pronounced, showing a steady

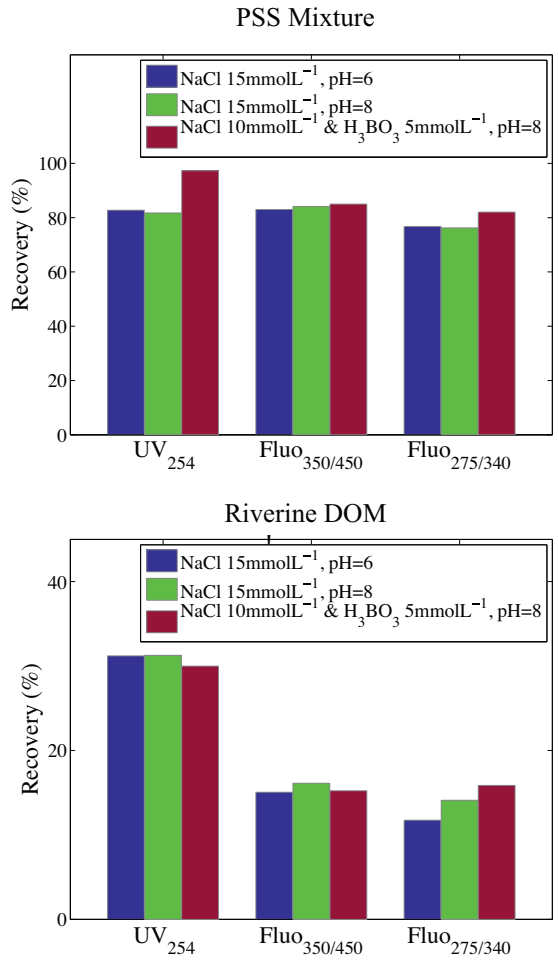

Fig. 7. Effects of carrier solutions on the recovery of colloidal DOM in chromophoric (UV_{254}), humic-like ($Fluo_{350/450}$) and protein-like ($Fluo_{275/340}$) substances in the PSS mixture and a riverine DOM sample.

increase from 11.7% with Carrier 1 to 14.5% and 15.9% with Carriers 2 and 3, respectively (Fig. 7).

Furthermore, carrier solutions also affected the elution time of samples from the AFlFFF channel. In the PSS mixture, chromophoric, humic-like and protein-like DOM all showed a steady decrease in elution time when the carrier solution was changed from Carriers 1 to 2 and 3 (Fig. 8). In the natural DOM sample, although to a smaller extent, chromophoric and humic-like DOM both were eluted earlier using carriers 2 and to 3 (Fig. 8). Protein-like DOM seemed to be eluted earlier when the carrier solution was changed from Carrier 1 to Carrier 2, but elution time increased from Carrier 2 to Carrier 3 (Fig. 8). Data from online-coupled multi-angle laser-light scattering detector were used to determine the radius of gyration (R_g) at peak intensities of each DOM component in the riverine DOM sample (Table 7). For all three DOM components (chromophoric, humic-like and protein-like), their peak R_g decreased from Carrier 1 to Carrier 2 and then increased to the highest value for Carrier 3. For example, the peak R_g value was 1.66, 1.51 and 1.99 nm for Carriers 1, 2 and 3, respectively, for humic-like DOM (Table 7).

Table 7
Detected radius of gyration from on-line coupled multi-angle light scattering (MALS) detector at peaks of the UV and fluorescence detectors.

	Rg (nm)		
	UV_{254}	$Fluo_{350/450}$	$Fluo_{275/340}$
Carrier 1	1.28	1.66	1.73
Carrier 2	1.27	1.51	1.65
Carrier 3	1.38	1.99	2.07

Previous studies have investigated the effect of matrix, ionic strength and pH of carrier solutions on the changes of recovery and elution time of colloidal materials through changes of interactions of colloidal materials between themselves and with the membrane [31,50,51,36]. As pH of the carrier solution increases, the surfaces of PSS standards and natural DOM and the membrane may become more negatively charged, increasing the repulsion between sample analytes and the membrane. Thus, sample analytes could be distributed further away from the membrane and more toward the center of the channel where the laminar channel flow is faster, resulting in decreased retention time and decreased adsorption of colloids onto the membrane, and hence increased recovery [31,52,50]. Therefore, when the carrier solution was changed from Carrier 1 to 2, pH increased from 6 to 8, leading to higher recovery and earlier elution. In addition, it has been shown that lower ionic strength would result in an increase in the electric double layer of colloids and lead to the positioning of colloids further away from the membrane [53,50,54]. Thus, this electrostatic influence may cause shorter retention time and higher recovery [36]. Carriers 1 and 2 had ionic strengths of 15 mM, while Carrier 3 had a lower ionic strength of ~10.3 mM. Highest R_g at peak positions were found with Carrier 3, consistent with the increased electric double layer at lower ionic strength. The faster elution of PSS standards and chromophoric and humic-like DOM using Carrier 3 likely resulted from the repulsive effect between analytes and the membrane, and hence further position from the membrane with faster laminar flow rate and earlier elution. Interestingly, protein-like DOM in the riverine DOM sample was eluted slightly later using Carrier 3 compared to Carrier 2, but with higher recovery. Proteins (e.g., BSA) have been found to have increased adsorption to membrane with decreased ionic strength when pH is at its isoelectric point (IEP) [51]. It is possible that proteins with IEP close to the pH of the carrier solution (~8) dominantly caused longer retention time and slower elution of protein-like DOM in samples.

For the measurement of natural DOM, carrier solutions with pH of 7–8.5 and moderate ionic strength (10–16 mM) have been shown to provide optimum recovery and separation [31,50,36]. Buffer solutions have also been widely used as carrier solutions [15,25,29]. It seems that Carrier 3 (borate buffer and pH 8) provided the highest recovery and reasonable separation and is thus recommended for separation and characterization of natural DOM samples although theoretically the specific sample's innate ionic strength and pH should be referred to when preparing carrier solution, especially for estuarine water samples with different salinities.

3.6. Fluorescence EEMs of different DOM size ranges

Using a 3-D fluorescence spectrophotometer, fluorescence EEMs of selected size fractions collected by a fraction collector were characterized and compared to the signatures from online detectors. Results of the SDOM-B sample served as an example here. From online coupled UV and fluorescence detectors, the fractograms of the three major groups of DOM were exhibited in Fig. 9: including the dominant group at the 0.5–4 nm, containing all the chromophoric, humic-like and protein-like DOM components; the second group at the 4–8 nm with mostly protein-like DOM; and the third group corresponding to the >55 nm (55–700 nm) with almost exclusive presence of protein-like DOM.

The fluorescence EEMs of the three DOM fractions at size intervals of 0.5–4 nm, 4–8 nm, and >55 nm are shown in Fig. 9(upper right panels), along with the fractograms of UV_{254}, $Fluo_{350/350}$ and $Fluo_{275/340}$. The EEM of the bulk DOM is also included for comparisons to show the heterogeneous compositions among different

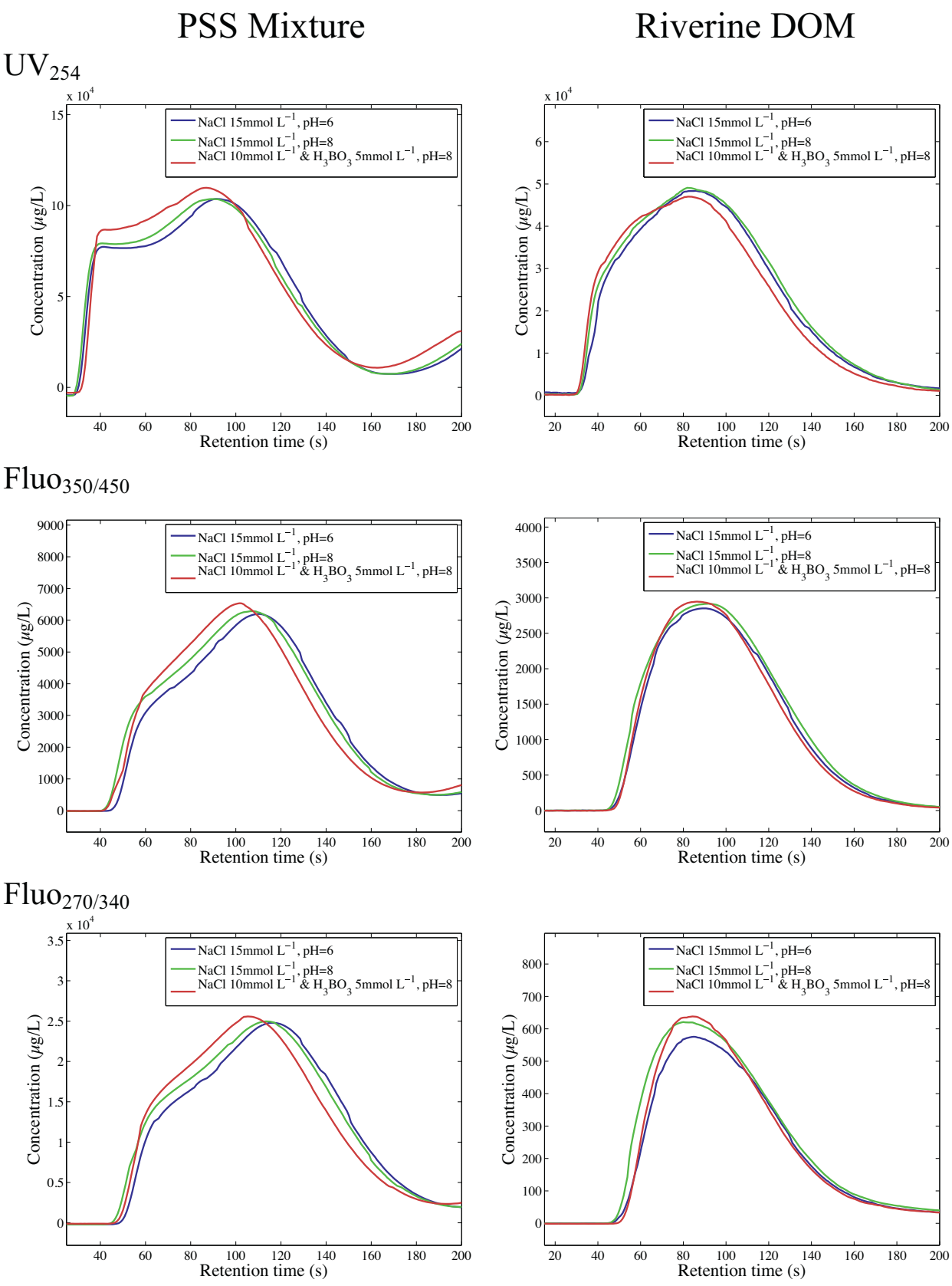

Fig. 8. Effects of carrier solutions on the fractograms of chromophoric (UV_{254}), humic-like ($Fluo_{350/450}$) and protein-like ($Fluo_{275/340}$) substances in the PSS mixture and a riverine DOM sample.

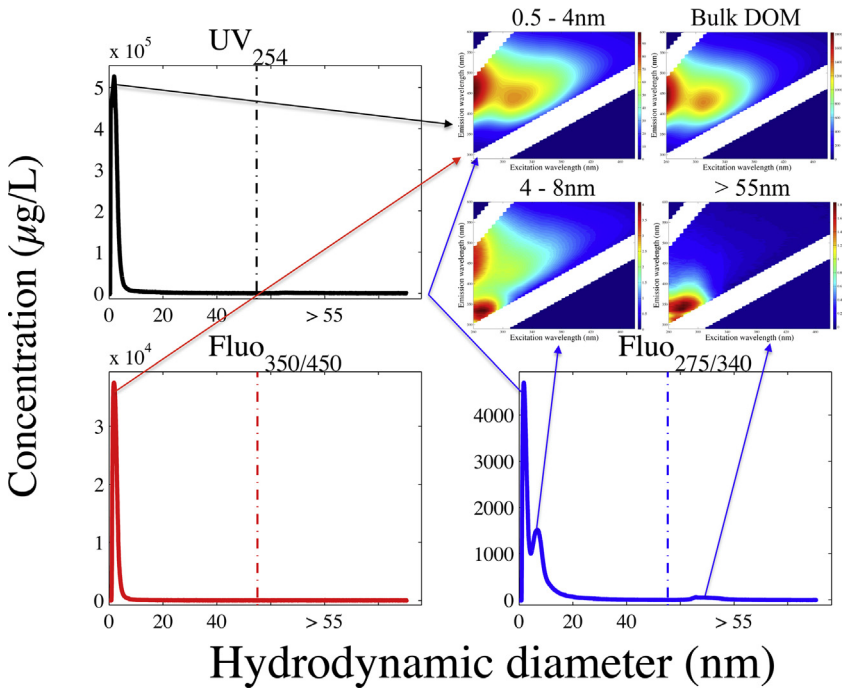

Fig. 9. Fractograms of a soil DOM sample based on data measured by online detectors including UV-absorbance (UV_{254}), fluorescence at Ex/Em 350/450 nm ($Fluo_{350/450}$), and fluorescence at Ex/Em 275/350 nm ($Fluo_{275/340}$). Also shown in the upper right panels are the fluorescence EEMs of different DOM size fractions at the 0.5–4 nm, 4–8 nm and the >55 nm as well as the bulk DOM sample.

sized DOM (Fig. 9). In addition to dominant humic-like signatures in Peaks A (Ex/Em 260/380–460 nm, UV humic-like) and C (Ex/Em 320–360/420–480 nm, terrestrial humic-like), it also exhibited protein-like signatures in Peaks B (Ex/Em 230,275/305–310 nm, tyrosine-like) and T (Ex/Em 230,275/340 nm, tryptophan-like) although at low intensities (Fig. 9). The EEMs of the three size fractions clearly show a distinction in chemical composition between different DOM size fractions (Fig. 9). DOM at the 0.5–4 nm showed great resemblance to the bulk DOM in their fluorescence EEMs with contributions mainly from the humic-like DOM, matching the results from the fractograms and consistent with the conclusion that the 0.5–4 nm DOM was the predominant component of the bulk DOM (Table 6). Fluorescence EEMs of the 4–8 nm DOM fraction had a significantly lower overall intensity, indicating fewer moieties of fluorescent materials, but significantly higher importance of Peaks B and T, showing more protein-like components in this size range. This matches the results from the on-line coupled fluorescence detector at Ex/Em 350/450 nm and indicated limited amount of terrestrial humic-like DOM in the 4–8 nm size fraction. In addition, Peak A showed higher intensity than Peak C and similar importance as Peaks B and T, showing the presence of UV humic-like DOM at the 4–8 nm size fraction. However, this was not captured by the on-line coupled detectors since they were not set at the specific Ex/Em pair for Peak A. Fluorescence EEM of the >55 nm DOM had even lower overall fluorescence intensity (Fig. 9), indicating that most fluorescent materials are partitioned to the <55 nm size range as shown in Table 6. However, the strong presence of Peak T and also Peak B in the EEMs (Fig. 9) indicated that the >55 nm DOM contained mostly protein-like components, matching findings from on-line coupled detectors (Fig. 9).

The characteristics of DOM at different size ranges derived from EEMs measured off-line matched those from online-coupled detectors set at specific Ex/Em pairs, and additionally provided more detailed information of DOM composition in different size fractions. Off-line coupling with other detectors could thus provide complementary information although on-line coupling of FlFFF with detectors has greatly advanced our understanding of aquatic colloids and nanoparticles.

4. Conclusions

The effect of membrane's MW cutoff and carrier solutions on the retention characteristics, recovery, and size distribution of macromolecules and natural DOM samples were systematically evaluated on an AFlFFF system. PSS standards and Rhodamine B were used to determine their recoveries by various membranes with different NMWCOs in the AFlFFF system. The recovery rate of macromolecules from the AFlFFF increased with increasing MWs. The apparent NMWCOs of three membranes derived from a >90% recovery rate had been determined as 1.9 kDa for the 0.3 kDa membrane, 2.7 kDa for the 1 kDa membrane, and 33 kDa for the 10 kDa membrane, respectively, all significantly larger than their respective manufacturer's rated NMWCOs.

After membrane calibration, three natural DOM samples and a PSS mixture sample were used to examine the influence of membrane's NMWCO and carrier solutions on the determined colloidal size distribution. Fractograms of soil DOM samples show a predominant colloidal size partitioning to the <5 nm size fraction, consistent with the size characteristics of humic substances. Fractograms of DOM samples using the 1 kDa and 10 kDa membranes were only a subset of that recovered by the 0.3 kDa membrane. In addition, soil DOM recovery rate by the AFlFFF decreased significantly with increasing membrane's NMWCO, from 45% with the 0.3 kDa membrane to 2–3% with the 10 kDa membrane for chromophoric DOM component quantified from $UV_{254\,nm}$. Integrated recovery at different DOM size intervals showed that the loss of materials at the 0.5–5 nm size range was mainly responsible for the decline in DOM recovery. Since the molecular size of natural DOM is mostly in the 1–3 kDa size range, the 0.3 kDa membrane is highly recommended for colloidal size characterization of natural DOM samples. The recovery or retention rate and elution time of DOM samples were closely related to the matrix, pH and ionic strength

of carrier solutions. Among the three carrier solutions tested, the borate buffer with pH of 8 seemed to provide the highest recovery and optimal separation for all DOM components, and is recommended as an optimal carrier solution for the characterization of natural DOM.

Rigorous calibration with macromolecular standards and optimization of experimental conditions are a prerequisite for quantifying colloidal size distribution and understanding the recovery and separation of natural DOM samples on any AFlFFF system. Off-line coupling with fluorescence EEMs technique could provide complementary DOM characterization at different colloidal size ranges.

Acknowledgements

We would like to thank Dr. Soheyl Tadjiki for his technical assistance and two anonymous reviewers for constructive comments, which improved the manuscript. This work was supported in part by grants from National Science Foundation-Major Research Instrument (NSF-OCE#1233192 to L.G.) and RGI and startup from University of Wisconsin-Milwaukee.

References

[1] J.I. Hedges, Why dissolved organic matter? in: D.A. Hansell, C.A. Carlson (Eds.), Biogeochemistry of Marine Dissolved Organic Matter, Academic Press, San Diego/London, UK, 2002, pp. 1–33.
[2] O.S. Pokrovsky, B. Dupré, J. Schott, Fe-Al-organic colloids control of trace elements in peat soil solutions: results of ultrafiltration and dialysis Aquat. Geochem. 11 (2005) 241–278.
[3] C. Lamelas, V.I. Slaveykova, Comparison of Cd(II), Cu(II), and Pb(II) biouptake by green algae in the presence of humic acid, Environ. Sci. Technol. 41 (2007) 4172–4178.
[4] V.I. Slaveykova, Predicting Pb bioavailability to freshwater microalgae in the presence of fulvic acid: algal cell density as a variable, Chemosphere 69 (2007) 1438–1445.
[5] J.E. Bauer, W.-J. Cai, P.A. Raymond, T.S. Bianchi, C.S. Hopkinson, P.A.G. Regnier, The changing carbon cycle of the coastal ocean, Nature 504 (2013) 61–70.
[6] L. Guo, J.K. Lehner, D.M. White, D.S. Garland, Heterogeneity of natural organic matter from the Chena River, Alaska, Water. Res. 37 (2003) 1015–1022.
[7] C. Guéguen, D.C. Burns, A. McDonald, B. Ring, Structural and optical characterization of dissolved organic matter from the lower Athabasca River, Canada, Chemosphere 87 (2012) 932–937, http://dx.doi.org/10.1016/j.chemosphere.2012.1001.1047
[8] R. Benner, R.M.W. Amon, The size-reactivity continuum of major bioelements in the ocean, Ann. Rev. Mar. Sci. 7 (2015), http://dx.doi.org/10.1146/annurev-marine-010213-135126
[9] L. Guo, P.H. Santschi, S.M. Ray, Metal partitioning between colloidal and dissolved phases and its relation with bioavailability to American oysters, Mar. Environ. Res. 54 (2002) 49–64.
[10] M. Chen, W.-X. Wang, L. Guo, Phase partitioning and solubility of iron in natural seawater controlled by dissolved organic matter, Glob. Biogeochem. Cycles. 18 (2004) GB4013.
[11] J.R. Lead, K.J. Wilkinson, Aquatic colloids and nanoparticles: current knowledge and future trends, Environ. Chem. 3 (2006) 159–171.
[12] L. Guo, P.H. Santschi, Ultrafiltration and its applications to sampling and characterisation of aquatic colloids, in: K.J. Wilkinson, J.R. Lead (Eds.), Environmental Colloids and Particles, John Wiley and Sons, Ltd, 2007, pp. 159–221, http://dx.doi.org/10.1002/9780470024539.ch9780470024534
[13] O.S. Pokrovsky, L.S. Shirokova, S.A. Zabelina, T.Y. Vorobieva, O.Y. Moreva, S.I. Klimov, A.V. Chupakov, N.V. Shorina, N.M. Kokryatskaya, S. Audry, J. Viers, C. Zoutien, R. Freydier, Size fractionation of trace elements in a seasonally stratified boreal lake: control of organic matter and iron colloids, Aquat. Geochem. 18 (2012) 115–139.
[14] J.C. Giddings, Field-flow fractionation: analysis of macromolecular, colloidal, and particulate materials, Science 260 (1993) 1456–1465.
[15] R. Beckett, Z. Jue, J.C. Giddings, Determination of molecular weight distributions of fulvic and humic acids using flow field-flow fractionation, Environ. Sci. Technol. 21 (1987) 289–295.
[16] M.A. Benincasa, J.C. Giddings, Separation and molecular weight distribution of anionic and cationic water-soluble polymers by flow field-flow fractionation, Anal. Chem. 64 (1992) 790–798.
[17] E. Alasonati, B. Stolpe, M.-A. Benincasa, M. Hassellöv, V.I. Slaveykova, Asymmetrical flow field flow fractionation - multidetection system as a tool for studying metal–alginate interactions, Environ. Chem. 3 (2006) 192–198.
[18] M. Baalousha, F.V.D. Kammer, M. Motelica-Heino, H.S. Hilal, P. Le Coustumer, Size fractionation and characterization of natural colloids by flow-field flow fractionation coupled to multi-angle laser light scattering, J. Chromatogr. A 1104 (2006) 272–281.
[19] M. Baalousha, B. Stolpe, J.R. Lead, Flow field-flow fractionation for the analysis and characterization of natural colloids and manufactured nanoparticles in environmental systems: a critical review, J. Chromatogr. A 1218 (2011) 4078–4103.
[20] B. Stolpe, L. Guo, A.M. Shiller, G.R. Aiken, Abundance, size distributions and trace-element binding of organic and iron-rich nanocolloids in Alaskan rivers, as revealed by field-flow fractionation and ICP-MS, Geochim. Cosmochim. Acta 105 (2013) 221–239.
[21] E. Bolea, M.P. Gorriz, M. Bouby, F. Laborda, J.R. Castillo, H. Geckeis, Multielement characterization of metal-humic substances complexation by size exclusion chromatography, asymmetrical flow field-flow fractionation, ultrafiltration and inductively coupled plasma-mass spectrometry detection: a comparative approach, J. Chromatogr. A 1129 (2006) 236–246.
[22] A.D. Pifer, D.R. Miskin, S.L. Cousins, J.L. Fairey, Coupling asymmetric flow-field flow fractionation and fluorescence parallel factor analysis reveals stratification of dissolved organic matter in a drinking water reservoir, J. Chromatogr. A 1218 (2011) 4167–4178.
[23] C.W. Cuss, C. Guéguen, Determination of relative molecular weights of fluorescent components in dissolved organic matter using asymmetrical flow field-flow fractionation and parallel factor analysis, Anal. Chim. Acta 733 (2012) 98–102, http://dx.doi.org/10.1016/j.aca.2012.1005.1003
[24] R.D. Vaillancourt, W.M. Balch, Size distribution of marine submicron particles determined by flow field-flow fractionation, Limnol. Oceanogr. 45 (2000) 485–492.
[25] M. Hassellöv, Relative molar mass distributions of chromophoric colloidal organic matter in coastal seawater determined by flow field-flow fractionation with UV absorbance and fluorescence detection, Mar. Chem. 94 (2005) 111–123.
[26] B. Stolpe, Z. Zhou, L. Guo, A.M. Shiller, Colloidal size distribution of humic- and protein-like fluorescent organic matter in the northern Gulf of Mexico, Mar. Chem. 164 (2014) 25–37, http://dx.doi.org/10.1016/j.marchem.2014.1005.1007
[27] M. Hassellöv, B. Lyvén, C. Haraldsson, W. Sirinawin, Determination of continuous size and trace element distribution of colloidal material in natural water by on-line coupling of flow field-flow fractionation with ICPMS, Anal. Chem. 71 (1999) 3497–3502.
[28] B. Stolpe, L. Guo, A.M. Shiller, M. Hassellöv, Size and composition of colloidal organic matter and trace elements in the Mississippi River, Pearl River and the northern Gulf of Mexico, as characterized by flow field-flow fractionation, Mar. Chem. 118 (2010) 119–128.
[29] S. Dubascoux, F. Von Der Kammer, I. Le Hécho, M.P. Gautier, G. Lespes, Optimisation of asymmetrical flow field flow fractionation for environmental nanoparticles separation, J. Chromatogr. A 1206 (2008) 160–165.
[30] Y.-P. Chin, G. Aiken, E. O'Loughlin, Molecular weight, polydispersity, and spectroscopic properties of aquatic humic substances, Environ. Sci. Technol. 28 (1994) 1853–1858.
[31] M.E. Schimpf, M.P. Petteys, Characterization of humic materials by flow field-flow fractionation, Colloid. Surf. A. 120 (1997) 87–100.
[32] C. Guéguen, C.W. Cuss, Characterization of aquatic dissolved organic matter by asymmetrical flow field-flow fractionation coupled to UV–visible diode array and excitation emission matrix fluorescence, J. Chromatogr. A 1218 (2011) 4188–4198, http://dx.doi.org/10.1016/j.chroma.2010.4112.4038, 41.
[33] M.S. Jiménez, M.T. Gómez, E. Bolea, F. Laborda, J. Castillo, An approach to the natural and engineered nanoparticles analysis in the environment by inductively coupled plasma mass spectrometry, Int. J. Mass. Spectrom. 307 (2011) 99–104.
[34] Q. Du, M.E. Schimpf, Correction for particle–wall interactions in the separation of colloids by flow field-flow fractionation, Anal. Chem. 74 (2002) 2478–2485.
[35] H. Hadri, J. Gigault, P. Chéry, M. Potin-Gautier, G. Lespes, Optimization of flow field-flow fractionation for the characterization of natural colloids, Anal. Bioanal. Chem. (2013) 1–11.
[36] E. Neubauer, F.V.D. Kammer, T. Hofmann, Influence of carrier solution ionic strength and injected sample load on retention and recovery of natural nanoparticles using flow field-flow fractionation, J. Chromatogr. A 1218 (2011) 6763–6773.
[37] M.L. Wells, The colloidal size spectrum of CDOM in the coastal region of the Mississippi Plume using flow field-flow fractionation, Mar. Chem. 89 (2004) 89–102, http://dx.doi.org/10.1016/j.marchem.2004.1002.1009
[38] S.A. Floge, M.L. Wells, Variation in colloidal chromophoric dissolved organic matter in the Damariscotta Estuary, Maine, Limnol. Oceanogr. 52 (2007) 32–45.
[39] Z. Zhou, B. Stolpe, L. Guo, A.M. Shiller, Colloidal size distribution of dissolved organic matter in riverine and estuarine waters of the northern Gulf of Mexico as characterized by flow field-flow fractionation, Geochim. Cosmochim. Acta (2015) (submitted for publication).
[40] L. Guo, P.H. Santschi, A critical evaluation of the cross-flow ultrafiltration technique for sampling colloidal organic carbon in seawater, Mar. Chem. 55 (1996) 113–127.
[41] M. Cheryan, Ultrafiltration and Microfiltration Handbook, Technomic, Lancaster, PA, 1998.
[42] E. Zanardi-Lamardo, C.A. Moore, R.G. Zika, Seasonal variation in molecular mass and optical properties of chromophoric dissolved organic material in coastal waters of southwest Florida, Mar. Chem. 89 (2004) 37–54.
[43] Z. Zhou, L. Guo, A.M. Shiller, S.E. Lohrenz, V.L. Asper, C.L. Osburn, Characterization of oil components from the Deepwater Horizon oil spill in the Gulf

of Mexico using fluorescence EEM techniques, Mar. Chem. 148 (2013) 10–21, http://dx.doi.org/10.1016/j.marchem.2012.1010.1003
[44] K.O. Buesseler, J.E. Bauer, R.F. Chen, T.I. Eglinton, O. Gustafsson, W. Landing, K. Mopper, S.B. Moran, P.H. Santschi, R. VernonClark, M.L. Wells, An intercomparison of cross-flow filtration techniques used for sampling marine colloids: overview and organic carbon results, Mar. Chem. 55 (1996) 1–31.
[45] L. Lin, Y. Cai, X. Sun, M. Chen, On the integrity of a commercial cassette ultrafiltration membrane: implications for marine colloidal biogeochemistry, Acta. Oceanol. Sin. 33 (2014) 109–116.
[46] L. Guo, P.H. Santschi, K.W. Warnken, Dynamics of dissolved organic carbon (DOC) in oceanic environments, Limnol. Oceanogr. 40 (1995) 1392–1403.
[47] G.R. Aiken, H. Hsu-Kim, J.N. Ryan, Influence of dissolved organic matter on the environmental fate of metals, nanoparticles, and colloids, Environ. Sci. Technol. 45 (2011) 3196–3201, http://dx.doi.org/10.1021/es103992s
[48] O.S. Pokrovsky, J. Schott, B. Dupré, Trace element fractionation and transport in boreal rivers and soil porewaters of permafrost-dominated basaltic terrain in Central Siberia, Geochim. Cosmochim. Acta 70 (2006) 3239–3260.
[49] M. Baalousha, J.R. Lead, Characterization of natural aquatic colloids (<5 nm) by flow-field flow fractionation and atomic force microscopy, Environ. Sci. Technol. 41 (2007) 1111–1117.
[50] M.H. Moon, I. Park, Y. Kim, Size characterization of liposomes by flow field-flow fractionation and photon correlation spectroscopy: effect of ionic strength and pH of carrier solutions, J. Chromatogr. A 813 (1998) 91–100.
[51] K.L. Jones, C.R. O'Melia, Protein and humic acid adsorption onto hydrophilic membrane surfaces: effects of pH and ionic strength, J. Membrane. Sci. 165 (2000) 31–46.
[52] M.E. Schimpf, K.-G. Wahlund, Asymmetrical flow field-flow fractionation as a method to study the behavior of humic acids in solution, J. Microcolumn. Sep. 9 (1997) 535–543.
[53] M.H. Moon, Effect of carrier solutions on particle retention in flow field-flow fractionation, Bull. Kor. Chem. Soc. 16 (1995) 613–619.
[54] E. Alasonati, M.-A. Benincasa, V.I. Slaveykova, Asymmetrical flow field-flow fractionation coupled to multiangle laser light scattering detector: optimization of crossflow rate, carrier characteristics, and injected mass in alginate separation, J. Sep. Sci. 30 (2007) 2332–2340.